Published in final edited form as:
Traffic. 2009 May ; 10(5): 590–599. doi:10.1111/j.1600-0854.2009.00894.x.

Discovery of New Cargo Proteins that enter Cells through Clathrin-Independent Endocytosis

Craig A. Eyster[*,£], **Jason D. Higginson**[*,£], **Robert Huebner**[*,£], **Natalie Porat-Shliom**[*,≠], **Roberto Weigert**[§], **Wells W. Wu**[¶], **Rong-Fong Shen**[¶], and **Julie G. Donaldson**[*]

[*]Laboratory of Cell Biology National Institutes of Health, Bethesda, Maryland 20892

[¶]Proteomics Core Facility, NHLBI National Institutes of Health, Bethesda, Maryland 20892

[§]Oral and Pharyngeal Cancer Branch, NIDCR, National Institutes of Health, Bethesda, Maryland 20892

[≠]Department of Neurobiochemistry, Tel Aviv University, Tel Aviv, Israel

Abstract

Clathrin-independent endocytosis (CIE) allows internalization of plasma membrane proteins lacking clathrin-targeting sequences, such as the major histocompatibility complex Class I protein (MHCI), into cells. After internalization, vesicles containing MHCI fuse with transferrin-containing endosomes generated from clathrin-dependent endocytosis. In HeLa cells, MHCI is subsequently routed to late endosomes or recycled back out to the plasma membrane (PM) in distinctive tubular carriers. Arf6 is associated with endosomal membranes carrying CIE cargo and expression of an active form of Arf6 leads to the generation of vacuolar structures that trap CIE cargo immediately after endocytosis, blocking the convergence with transferrin-containing endosomes. We isolated these trapped vacuolar structures and analyzed their protein composition by mass spectrometry. Here we identify and validate six new endogenous cargo proteins (CD44, CD55, CD98, CD147, Glut1 and ICAM1) that use CIE to enter cells. CD55 and Glut1 appear to closely parallel the trafficking of MHCI, merging with transferrin endosomes before entering the recycling tubules. In contrast, CD44, CD98 and CD147 appear to directly enter the recycling tubules and by-pass the merge with EEA1-positive, transferrin-containing endosomes. This divergent itinerary suggests that sorting may occur along this CIE pathway. Furthermore, the identification of new cargo proteins will assist others studying CIE in different cell types and tissues.

Keywords

clathrin-independent endocytosis; non-clathrin endocytosis; Glut1; emmprin; 4F2; glucose transporter 1; CD44; CD55; CD98; CD147; Arf6

Introduction

Cells bring extracellular fluids, nutrients, ligands, and plasma membrane proteins and lipids into the cell interior by the process of endocytosis. Once internalized, endosomal membrane and content are sorted and routed to late endosomes for degradation, to the trans Golgi network, or recycled back to the PM. Among the various forms of endocytosis, clathrin-

Corresponding author: Julie G. Donaldson, NHLBI, NIH, Bld 50, Rm 2503, Bethesda, MD, 20892, 301-402-2907 ph, 301-402-1519 fax, jdonalds@helix.nih.gov.
[£]These authors contributed equally to this work.

dependent endocytosis (CDE) has been the best characterized with regards to the machinery, regulation, and the cargo proteins that it carries (1). Cargo proteins that enter cells through CDE contain specific targeting sequences in their cytoplasmic domains capable of being recognized by adaptor proteins that sort them into clathrin coated vesicles. By contrast, there are proteins at the PM that lack adaptor protein-targeting sequences, and these proteins enter cells by clathrin-independent endocytosis (CIE). Recently, there has been increased interest in CIE and the subsequent routing of the internalized membrane and protein by these pathways (2,3). There is some evidence for distinct CIE pathways for different types of cargo and cells. However, these distinctions often have been based on following the endocytosis of transfected proteins or lipid-binding toxins into cells. For this reason, it has been difficult to compare these different pathways to see how typical they are in different cell types.

We and others have used HeLa cells as a model system to investigate how CIE is regulated and the subsequent trafficking of cargo molecules that enter cells through this mechanism (4). Endogenous proteins that enter cells through this mechanism have been identified including the major histocompatibility complex Class I (MHCI) protein (5,6), syndecan 1 (7), β1-integrin (8), the GPI-anchored protein CD59 (9), and the MHC-like molecule that presents lipids to T cells CD1a (10). In addition, other cargo proteins shown to traffic through this pathway in transfection experiments include E-cadherin (11), the major myelin protein PMP22 (12), potassium channels (13), the cation channel protein mucolipin-2 (14), the metabotropic glutamate receptor (15), the β2 adrenergic and M3 muscarinic receptors (16) and peptide-loaded MHC Class II (17). Once internalized, vesicles containing these cargo proteins fuse with endosomes containing cargo that entered through CDE and the cargo is then routed either to late endosomes and lysosomes for degradation or to distinct tubular endosomes that recycle membrane back to the PM.

CIE in Hela cells occurs independently of clathrin and dynamin but requires free cholesterol (5,9). Although little is known about the endocytic machinery that mediates the internalization step, there are a number of GTP-binding proteins that regulate the subsequent trafficking of the vesicles and cargo. One such GTPase is Arf6, which alters the cortical actin cytoskeleton and the lipid composition at the PM through activation of phosphatidylinositol 4-phosphate 5-kinase and phospholipase D (18,19). Arf6 is associated with the CIE pathway in HeLa cells and its proper functioning is required at two sites along the pathway. After internalization, Arf6-GTP undergoes hydrolysis leading to a change in the phosphoinositide composition of the endosome (20). Endosomal phosphatidylinositol 4,5-bisphosphate (PIP_2) is lost and phosphatidylinositol 3-phosphate (PI3P) is acquired to enable fusion of the endosome with the PI3P and Rab5-associated “classical” early endosome that contains clathrin cargo (5). Expression of a constitutively active form of Arf6, Arf6Q67L, stimulates CIE but leads to the accumulation of internalized cargo in enlarged vacuolar-type structures that are coated with actin and PIP_2. These Q67L vacuoles trap CIE cargo, but not CDE cargo such as transferrin and LDL receptors, and further traffic to Rab5 endosomes and recycling is blocked (5,9,20). On the other hand, Arf6 activation is required for the recycling from the tubular endosomal membrane back to the PM (6). In addition to Arf6, many other regulatory proteins have been shown to mediate this recycling including Rab11, Rab22 (21), Rab35 (17), the eps15 homology domain proteins EHD1 (22) and EHD3 (23), extracellular signal-regulated kinase Erk (24), Alix (25), Cdc42, and Par3 (26). The internalization of membrane and subsequent recycling, which can be directed to specific regions of the PM, might be a major function for this endosomal system. Indeed, this Arf6-mediated membrane recycling appears to be critical for many functions attributed to Arf6 including Rac ruffling, cell adhesion, cell migration and wound healing (18,19).

In the interest of identifying machinery responsible for endocytosis and new PM proteins that enter cells through CIE, we isolated the vacuolar membranes that accumulate in HeLa cells expressing Arf6Q67L in order to analyze their protein composition. Here we report on the proteomic analysis of enriched, CIE early endosomes that has led to the identification of new cargo proteins that travel in this pathway. These new proteins are associated with nutrient uptake and interactions of cells with the extracellular matrix, and unexpectedly, reveal an alternative intracellular trafficking route in the CIE pathway.

Results and Discussion

In order to isolate early endosomes originating from CIE we considered ways to affinity purify this endosomal compartment. In another study ongoing in the laboratory, we had identified PM SNARE proteins that travel along the CIE pathway. Expression of an amino terminally GFP-tagged syntaxin 3 localized to the PM and tubular endosomal membranes (Fig. 1A) that also contained internalized MHCI (not shown). GFP-syntaxin 3 also localized to the vacuolar membranes containing CIE cargo proteins that form in cells expressing Arf6Q67L (Fig. 1A) (5,9,20). Endogenous syntaxin 3, detected with a specific antibody, also localized to these endosomal membranes (not shown). Since the GFP tag was on the amino terminus of Syntaxin 3 and hence was exposed on the outer surface of the vacuoles, we decided to affinity purify these vesicles with antibodies to GFP.

Whole cell lysates from HeLa cells that had been transfected with Arf6Q67L and GFP-Syntaxin 3 were incubated with anti-GFP-coupled magnetic beads to pull-out GFP-containing membranes. Although the GFP-Syntaxin 3 in cells expressing Arf6Q67L was present both at the PM and on the vacuoles, experiments with disrupted cells that had been surface biotinylated indicated that the PM fragments would reseal with the extracellular surface out and so the GFP tag would not be available for immunoisolation. Material bound to the beads was resolved by electrophoresis and the proteins stained using a sensitive Coomassie staining technique (27). It was clear that there were many more proteins associated with the Anti-GFP beads than the IgG control beads (Fig. 1B). Slices of gels were made and digested with trypsin as described in Materials and Methods. The subsequent peptide fragments were subjected to LC-MS/MS for identification.

Among the proteins identified through this proteomic screen were 6 new membrane proteins that might represent new cargo molecules that travel along this CIE pathway. They are : CD44, CD55, CD98, CD147, the non-insulin stimulated glucose transporter 1 (Glut1), and the intercellular adhesion molecule 1 (ICAM1) (Fig. 1C). For three of these (CD98, CD147 and Glut1) we obtained antibodies able to recognize the endogenous protein in immunoblots. When the isolated membrane fractions were probed with these antibodies, bands representing CD98, CD147 and Glut1 were apparent in the fractions from the Anti-GFP beads and also in the whole cell lysate (Fig. 1D). MHCI, a protein known to follow this CIE pathway (5,6), also was identified in the proteomic analysis and we detected MHCI protein in the material bound to the anti-GFP-beads (Fig. 1D).

Next, we validated that these 6 membrane proteins were associated with the Arf6Q67L-generated vacuoles in cells by immunofluorescence. Hela cells were transfected with Arf6Q67L and a GFP-tagged membrane marker (Mem-GFP), composed of GFP with the carboxyl tail segment from H-Ras, which we have previously showed associates with membranes of the CIE pathway in HeLa cells (28). After transfection, the cells were fixed and then localization of the endogenous proteins was determined. With antibodies directed to each of the newly identified proteins, we observed that CD44, CD55, CD98, CD147, Glut1 and ICAM1 all colocalized with Mem-GFP on discrete vacuoles in the periphery (Fig.

2, insets) and on clustered vacuoles in the juxtanuclear region, typical of cells expressing Arf6Q67L (5,9,20).

An interesting aspect of these membrane proteins is that many of them either are nutrient transporters or are involved in regulating cellular interactions with the matrix, an activity that has been associated with Arf6-regulation of CIE pathway trafficking (18,19). CD44 is a cell adhesion molecule and receptor for hyaluronan, an extracellular glycosaminoglycan. It is believed to direct matrix metalloproteinases to the leading edge of cells (29). CD55, also known as decay acceleration factor (DAF) is a GPI-anchored protein as is CD59, which we previously identified as being associated with these endosomes. Both of these GPI-anchored proteins protect cells from complement-mediated lysis (30).

CD98 is a multifunctional protein that is responsible for nutrient uptake and interacts with proteins involved in cell-matrix interactions (31). It is the heavy chain of some amino acid transporters, in particular with Lat1, responsible for neutral amino acid transport. Although we also identified Lat1 in the proteomic analysis, we have not found an antibody suitable for immunolocalization. CD98 may also associate with Glut1, the ubiquitous glucose transporter, which we identified in the screen. CD98 also associates with β1-integrin, a previously identified cargo (8), and with CD147, which is a new cargo protein identified here. CD147, also known as Emmprin for extracellular matrix metalloproteinase inducer, associates with the monocarboxylate transporter proteins that transport lactate and pyruvate across the PM (32).

Having validated that these endogenous membrane proteins were in fact associated with the isolated vacuoles that were analyzed by mass spectroscopy, we next examined whether these proteins were present on CIE endosomes in untransfected cells. First, we observed that the total, steady state distribution of these cargo proteins colocalized with MHCI in HeLa cells (data not shown). Next, we used antibody internalization to assess whether these proteins followed a membrane trafficking pathway similar to that of MHCI and distinct from that of transferrin. We and others have previously shown that using monoclonal antibodies to follow the internalization of PM proteins does not alter their trafficking (5,9). The antibodies do not cause cross-linking of the proteins; in fact, for MHCI, cross-linking of the primary antibodies using secondary antibodies inhibits endocytosis (unpublished observations). After 60 min internalization, CD55 localization was almost identical to that of MHCI on punctate structures in the peripheral and juxtanuclear region some of which colocalized with transferrin (Fig. 3A). Additionally, CD55 and MHCI were both associated with the tubular, recycling endosomes that emanated from the juxtanuclear region that were devoid of transferrin (Fig. 3A, inset) and are characteristic for the CIE pathway in HeLa cells (21). Since we did not have antibodies that recognized the extracellular portion of Glut1, to follow Glut1 endocytosis, we transfected HeLa cells with a Glut1 construct with an extracellular HA tag (HA-Glut1) so we could examine internalization with anti-HA antibodies. After 60 min internalization, HA-Glut1 colocalized with the internalized MHCI on some perinuclear punctate structures that colocalized with transferrin and on tubular endosomes devoid of transferrin (Fig. 3A inset) as we observed with CD55. The distribution of HA-Glut1 was similar to that of endogenous Glut1, which colocalized with endocytosed MHCI on juxtanuclear endosomes and tubular recycling endosomes (Supp. Fig. 1). Although we could assess the steady state distribution of ICAM1 in cells by immunofluorescence (Fig. 2), we were unable to follow endocytosis of ICAM1 using the antibodies available.

In contrast to what we observed with CD55 and Glut1, CD44, CD98 and CD147 showed a different pattern of internalization. CD44 colocalized with MHCI on tubular endosomes but was not associated with MHCI in the juxtanuclear region nor did it colocalize with transferrin (Fig. 3B). CD98 and CD147 distributions were especially striking as they were

prominently associated with tubular endosomal membranes and absent in the juxtanuclear region where MHCI colocalized with transferrin (Fig. 3B inset). This different distribution after 60 min of internalization suggested some differences in itinerary for these new cargo proteins. To examine this more closely we followed the internalization of CD98 and MHCI over shorter periods of time. At 5 min, CD98 and MHCI were observed in the same punctate structures and then at 10 min CD98 was observed in tubular endosomes but MHCI did not appreciably reach these structures until 30 min (Fig. 4).

In addition to CD98, we noticed that CD44 and CD147 also appeared to gain access to the tubular endosome more rapidly than did MHCI, possibly by evading fusion with the common “classical” early endosome that contained transferrin, Rab5 and the early endosomal antigen 1 (EEA1). To test this possibility, we examined whether internalized cargo proteins reached endosomes that labeled with EEA1. After 30 min internalization, CD55 and HA-Glut1 were observed in puncta in the juxtanuclear region that colocalized with EEA1, similar to that of MHCI (Fig. 5A), as we have reported previously (5). In contrast, internalized CD44, CD98 and CD147 were predominantly associated with endosomal tubules and vesicles that were devoid of EEA1 (Fig. 5B). These findings indicate that CD44, CD98 and CD147 largely avoid whereas CD55, Glut1 and MHCI readily reach EEA1- and transferrin-containing early endosomes. Thus, although all cargo proteins entered by CIE and became trapped in Arf6Q67L-associated endosomes, CD44, CD98 and CD147 appeared to by-pass EEA1 and transferrin-containing endosomes on their way to the tubular recycling endosome.

Since the itinerary of some of these new cargo proteins differed from that of MHCI, we followed the itinerary of CD98 in more detail to confirm that this new type of cargo protein was still utilizing the same CIE pathway that we had characterized for MHCI and CD59 (5,9,21). In particular, we examined whether internalization of CD98 was independent of dynamin and dependent on PM cholesterol and whether the trafficking of CD98 was altered upon expression of mutants of Rab22. Expression of the K44A mutant of dynamin2 did not affect internalization of CD98 or MHCI whereas transferrin internalization was inhibited (Supp. Fig. 2A). Additionally, treatment of cells with filipin to bind cell surface cholesterol (9) blocked internalization of CD98 (Supp. Fig. 2B) and MHCI as previously described (9). We previously showed that Rab22 is associated with the tubular recycling endosome associated with this CIE pathway in HeLa cells and that expression of the active mutant of Rab22 (Q64L) enhanced the tubular phenotype and also resulted in the accumulation of vesicles at the distal ends of the tubules (21). Furthermore, these tubules were absent in cells expressing the S19N dominant negative form of Rab22. We found that internalized CD98 and MHCI both colocalized with GFP-Rab22 and that in cells expressing Rab22Q64L there was an increase in number of cells exhibiting tubules and peripheral vesicles (Supp. Fig. 3) as we had observed previously for MHCI (21). Additionally in cells expressing Rab22S19N there was a marked decrease in number of cells exhibiting tubules and the internalized CD98 and MHCI colocalized in a perinuclear region of the cell (Supp. Fig. 3), which also contains transferrin receptor (21). Although our previous studies showed that expression of Rab22S19N inhibits recycling of MHCI but not that of transferrin (21), we were not able to quantitatively measure recycling of CD98 with the reagents at hand. We suspect, however that once in the tubular endosome, the recycling of the new cargo proteins is dependent upon the same components (Rab22, Rab11 and Arf6) that regulate recycling of MHCI (21).

Taken together, these PM proteins appear to be new CIE cargo that enter cells independently of dynamin, but dependent upon PM cholesterol and accumulate in Arf6Q67L vacuoles. Once inside the cell, however, the new cargo proteins revealed differences in their itineraries (Fig. 6). CD55 and Glut1 followed the same pathway as that of internalized MHCI (Fig. 6 Red Bars) and could be observed in endosomes that contain EEA1 and transferrin and then

later in the tubular recycling endosomes. This also appears to be the route traveled by CD59 (9), integrins (8) and syndecan (7). In contrast, CD44, CD98 and CD147 (Fig. 6 Green Bars) did not appear to enter the EEA1-positive compartment but appeared to join recycling tubular endosomes by way of the juxtanuclear endocytic recycling compartment (ERC). Previously we had observed evidence for this more direct recycling route taken by CD44, CD98 and CD147 when we were examining the distribution of Arf6, H-Ras and certain PM SNARE proteins. In HeLa cells these proteins are present on Arf6Q67L vacuoles and on the recycling tubules but never on enlarged, Rab5Q79L endosomes (5,9,28). We now have identified the cargo proteins that follow this direct pathway (CD44, CD98, CD147) in contrast to those cargo proteins that also merge with the EEA1 and Rab5 endosome (Glut1, CD55, CD59 and MHCI). We are in the process of identifying which features in cargo proteins might route them towards EEA1 compartments. Despite the different routes to the tubular endosome, both types of cargo are nonetheless trapped in the same structures, presumably the ERC, in cells expressing Rab22S19N.

The new CIE cargo proteins identified here join those already known and together they begin to reveal the physiological functions of this endocytic pathway. A number of these proteins (CD44, CD98, CD147, integrins and syndecan) are involved in cell-matrix interactions and are implicated in cell migration and metastasis. Another set of proteins are nutrient and ion transporters (CD98, CD147, Lat1, Glut1, potassium channels, mucolipin-2) or proteins that present themselves to the immune system (MHCI, Cd1a and MHCII). Additionally, we recently showed that the β2 adrenergic and M3 muscarinic receptors constitutively traffic along this CIE pathway and then upon ligand activation switch to internalization by clathrin pathways (16). The trafficking of these plasma membrane proteins and in particular recycling of these proteins to particular regions of the cell could have important consequences during development and for cell homeostasis. These proteins all lack known adaptor protein binding motifs but may contain other sequences in their trans-membrane or cytoplasmic regions that could interact with alternative coats or machinery used during CIE. With this new set of tools, we can examine CIE pathways and follow the trafficking of endogenous cargo proteins in different cell types to see how they are organized. These studies will likely reveal the range of CIE pathways in different cell types and provide insight into the cellular functions of such pathways.

Materials and Methods

Antibodies and Plasmids

Mouse monoclonal antibodies to MHCI from hybridoma cells, clones HC10 and w6/32 (IgG2a), were used for immunoblotting and immunofluorescence/internalization, respectively. Mouse monoclonal antibodies to CD44 (clone IM7; IgG2b), CD55 (clone JS11; IgG1), CD98 (clone MEM-108;IgG1), and CD147 (clone HIM6;IgG1) and Alexa fluor conjugated versions of these antibodies were purchased from BioLegend (San Diego, CA) and used for immunofluorescence and antibody internalization. We confirmed with another clone the internalization behavior for CD98 (clone UM7F8 from BD Pharmingen) and found a similar overall internalization pattern that also resembled localization of CD98 at steady state. Mouse antibody to ICAM1 (clone MEM-111) was purchased from BioLegend and was used for immunofluorescence. Goat anti-CD98 (Santa Cruz Biotechnology, Santa Cruz, CA) was used for immunoblotting. A rabbit polyclonal antibody to Glut1 (33) was kindly provided by Sam Cushman (NIH, Bethesda, MD) and used for immunolocalization. A rabbit antibody to Glut1 from Alpha Diagnostics (San Antonio, TX) was used for western blotting.

Arf6Q67L-FLAG construct was in pFLAG. A chimera of GFP and syntaxin 3 (GFP-syn3) was provided by Paul Roche (NIAID, NIH, Bethesda, MD). A plasmid encoding a GFP

chimera with the carboxyl terminal tail of H-Ras (Mem-GFP) that colocalizes with MHCI at the PM and on endosomal membranes (28) was from Clontech (Mountain View,CA). GFP-Rab22a wild type, S19N and Q64L were previously described (21).

Immuno-Bead Preparation

Protein A Dynabeads (Dynal Biotech, Oslo, Norway) were covalently cross-linked to affinity purified polyclonal rabbit anti-GFP (Invitrogen, Carlsbad, CA) antibody as recommended by the manufacturer. Control beads using rabbit IgG were handled in the same way. Prior to use, beads were washed one time with 0.1 M citrate (pH 3.1) and then three times with PBS containing 1 mg/ml soy bean trypsin inhibitor (PBS/STI).

Transfections

For transfection for proteomic analysis, HeLa cells were plated on 15-cm petri dishes for 1-2 days to achieve 50-70% confluence. HeLa cells were grown in DMEM supplemented with 10% FBS, 100 U/ml penicillin, and 100 μg/ml streptomycin at 37°C with 5% CO2. Cells were transfected with GFP-tagged syntaxin 3 (GFP-syn3) and Arf6-Q67L-FLAG using FuGene (Roche Diagnostics, Indianapolis, IN) as recommended by the manufacturer. Experiments were performed 10-12 h after transfection. The amount of cells grown (30 dishes) resulted in approximately 10 mg of cellular material. The vacuoles of interest were estimated to comprise 10 mg of the total cellular material.

Immunoisolation of GFP-Syn3 membranes

Cells were washed three times with cold PBS and harvested using a cell scraper at 4°C. The cells were collected and pelleted by centrifugation at 4°C (1200 × *rpm* for 5 min). Pellets were resuspended in 2 ml of homogenization buffer (HB) (HEPES 25mM, KCl 100mM, 1mM EDTA, pH 7.4 with protease inhibitor cocktail (PI) added). The cells were disrupted with 15 passes in a tight fitting glass homogenizer followed by sonication using 3 discontinuous applications of 10 sec each. The lysate was centrifuged at 4°C (800 *g* for 5 min). The post-nuclear supernatant (PNS) was removed and a small portion was analyzed for protein content (BioRad, Hercules, CA). Dynal immunoisolation beads, prepared as discussed above, were washed with 0.1 M citrate (pH 3.1) followed by 2 washings with (1ml) PBS/STI and then resuspended in this solution. The PNS was split between control (IgG) beads and anti-GFP beads. The binding conditions were consistent with Dynal Biotech's recommendations of 10 - 200 μg target per 1 mg of beads. The mixture was incubated at 4 °C for 1 h with continuous rotational mixing. After binding the beads were washed with PBS/STI three times at 4°C. The supernatant was discarded and proteins were eluted and solubilized by addition of 100 μl Laemmli sample buffer, followed by heating to 95°C for 10 minutes.

Separation by 1-D SDS-PAGE gel and trypsinization

Immunoisolated vacuoles were separated by SDS-PAGE using polyacrylamide minigels with a 4-20% gradient (BioRad Laboratories, Hercules, CA). Gels were then stained for 10 min with 0.01% Coomassie blue R250 (Sigma B-7920) in 50% methanol and 10% acetic acid (Luo et al 2006). The gels were then rinsed with 40% methanol and 7% acetic acid, followed by destaining for 10 min in the same solution, soaked for 5 minutes in water twice. Gels were visualized using an Odyssey infrared scanner (Li-Cor, Lincoln, NE). For the proteomic analysis, the entire lane of the gel was cut into sequential slices of approximately 1 mm thickness. Each of the slices was then destained using 25 mM NH_4HCO_3/50% acetonitrile (ACN) for ten-minute intervals until completely destained. Gel samples were then dried, reduced with 10 mM DTT in 25 mM NH_4HCO_3 for 1 hr at 56°C, and alkylated with 55 mM iodoacetamide in 25 mM NH_4HCO_3 for 45 min at room temperature in

darkness. Upon supernatant removal, the gels were washed with 25 mM NH_4HCO_3 for 10 min and with 25 mM NH_4HCO_3/50%ACN, and then dried. Proteins in gels were trypsinized using 12.5 ng/μl sequencing-grade modified trypsin (Promega, Madison, WI) diluted in 25 mM NH_4HCO_3 and incubated at 37°C for 16 hrs. Peptides were collected from digest solutions and gels were further extracted by sonication in a 50% ACN/5% formic acid solution and combined with corresponding digest solutions. Peptides in digest solutions were then lyophilized to near dryness and reconstituted with 15 μl 0.1% formic acid.

Nanospray LC/MS/MS analyses of tryptic peptides were carried out using a linear ion trap LTQ (Thermo Finnigan, San Jose, CA), as previously described (34). Briefly, peptides were first loaded onto a trap cartridge (Agilent, Palo Alto, CA) at a flow rate of 2 μl/min. Trapped peptides were then eluted onto a reversed-phase PicoFrit column (New Objective, Woburn, MA) using a linear gradient of ACN (0-60%) containing 0.1% formic acid. The duration of the gradient was 35 min at a flow rate of 0.25 μL/min, which was followed by 80% ACN washing for 5 minutes. The eluted peptides from the PicoFrit column were sprayed into an LTQ mass spectrometer equipped with a nanospray ion source. The data-dependent acquisition mode was enabled, and each survey MS scan was followed by five MS/MS scans with dynamic exclusion option on. The spray voltage and ion transfer tube temperature were set at 1.8 kV and 160°C, respectively. The normalized collision energy was set at 35%.

Mass spectrometric data files were searched against the NCBI human Refseq protein forward and reversed sequence database (as of 3/1/2007) using BioWorks 3.2 software (ThermoFinnigan, San Jose, CA) based on SEQUEST algorithm, as described previously (35). The identified peptide sequences were initially qualified and filtered using the following threshold: 1) the cross-correlation scores (Xcorr) of matches were rank first and greater than 1.5, 2.0, and 2.5 for charge state +1, +2, and +3 peptide ions, respectively, 2) the uniqueness scores of matches (ΔCn) were higher than 0.08, and 3) the ranks of the preliminary scores (Rsp) were less than 10. Using these criteria, the false positive rates for peptide identification, estimated from reverse database searches, were less than 5%. After such filtering, only proteins identified by at least two peptides were considered as positive identifications

Immunofluorescence and Antibody internalization

Cells were plated on glass coverslips 24 h prior to use. For immunolocalization, cells were fixed for 10 min in 2% formaldehyde in PBS, rinsed in PBS and then incubated with primary antibodies in PBS/10% FCS in the presence of 0.2% saponin. Primary antibodies were either directly conjugated or visualized by incubation with Alexa fluor-conjugated, goat-anti-mouse and goat-anti-rabbit secondary antibodies (Invitrogen, Carlsbad, CA). For antibody internalization assays, cells were incubated in complete media in the presence of 10-20 μg/ml monoclonal antibodies at 37°C to allow endocytosis of the antibody. After internalization, surface antibody was removed by low pH, acid wash prior to fixation or by incubation of fixed cells with unlabelled goat anti-mouse IgG in the absence of saponin. The internalized antibody was subsequently revealed by incubation with secondary antibodies in the presence of saponin. In experiments where internalization of 594 or 633-transferrin was monitored, the cells were first incubated for 30 min in DMEM without serum but containing 0.5% BSA, and then transferrin and antibodies were added to this media. All images were obtained using a 510 LSM confocal microscope (Zeiss, Thornwood, NY) with a 63× Plan Apo objective and processed using Adobe Photoshop.

Supplementary Material

Refer to Web version on PubMed Central for supplementary material.

Acknowledgments

The authors would like to thank Mark Knepper and Trairak Psitikun (NHLBI) for help with the proteomic data, Sam Cushman (NIDDK) for Glut1 antibody and constructs, and Lee Ann Cohen and Ed Korn for comments on the manuscript. This work was supported by the Intramural Research Program of the National Heart, Lung and Blood Institute, NIH.

JDH was a fellow in the National Capitol Consortium Neonatal-Perinatal Fellowship Program, Department of Pediatrics, Uniformed Services University and National Naval Medical Center, Bethesda, MD 20814. For JDH, the views expressed in this article are those of the authors and do not reflect the official policy or position of the Department of the Navy, Department of Defense or the US Government.

References

1. Conner SD, Schmid SL. Regulated portals of entry into the cell. Nature. 2003; 422(6927):37–44. [PubMed: 12621426]
2. Mayor S, Pagano RE. Pathways of clathrin-independent endocytosis. Nat Rev Mol Cell Biol. 2007; 8(8):603–612. [PubMed: 17609668]
3. Sandvig K, Torgersen ML, Raa HA, van Deurs B. Clathrin-independent endocytosis: from nonexisting to an extreme degree of complexity. Histochem Cell Biol. 2008; 129(3):267–276. [PubMed: 18193449]
4. Donaldson JG, Porat-Shliom N, Cohen LA. Clathrin-independent endocytosis: a unique platform for cell signaling and PM remodeling. Cell Signal. 2009; 21(1):1–6. [PubMed: 18647649]
5. Naslavsky N, Weigert R, Donaldson JG. Convergence of Non-clathrin- and Clathrin-derived Endosomes Involves Arf6 Inactivation and Changes in Phosphoinositides. Mol Biol Cell. 2003; 14(2):417–431. [PubMed: 12589044]
6. Radhakrishna H, Donaldson JG. ADP-ribosylation factor 6 regulates a novel plasma membrane recycling pathway. J Cell Biol. 1997; 139(1):49–61. [PubMed: 9314528]
7. Zimmermann P, Zhang Z, Degeest G, Mortier E, Leenaerts I, Coomans C, Schulz J, N'Kuli F, Courtoy PJ, David G. Syndecan recycling is controlled by syntenin-PIP2 interaction and Arf6. Dev Cell. 2005; 9(3):377–388. [PubMed: 16139226]
8. Powelka AM, Sun J, Li J, Gao M, Shaw LM, Sonnenberg A, Hsu VW. Stimulation-dependent recycling of integrin beta1 regulated by ARF6 and Rab11. Traffic. 2004; 5(1):20–36. [PubMed: 14675422]
9. Naslavsky N, Weigert R, Donaldson JG. Characterization of a nonclathrin endocytic pathway: membrane cargo and lipid requirements. Mol Biol Cell. 2004; 15(8):3542–3552. [PubMed: 15146059]
10. Barral DC, Cavallari M, McCormick PJ, Garg S, Magee AI, Bonifacino JS, De Libero G, Brenner MB. CD1a and MHC Class I Follow a Similar Endocytic Recycling Pathway. Traffic. 2008; 9(9): 1446–1457. [PubMed: 18564371]
11. Paterson AD, Parton RG, Ferguson C, Stow JL, Yap AS. Characterization of E-cadherin Endocytosis in Isolated MCF-7 and Chinese Hamster Ovary Cells: The initial fate of unbound E-cadherin. J Biol Chem. 2003; 278(23):21050–21057. [PubMed: 12657640]
12. Chies R, Nobbio L, Edomi P, Schenone A, Schneider C, Brancolini C. Alterations in the Arf6-regulated plasma membrane endosomal recycling pathway in cells overexpressing the tetraspan protein Gas3/PMP22. J Cell Sci. 2003; 116(Pt 6):987–999. [PubMed: 12584243]
13. Gong Q, Weide M, Huntsman C, Xu Z, Jan LY, Ma D. Identification and characterization of a new class of trafficking motifs for controlling clathrin-independent internalization and recycling. J Biol Chem. 2007; 282(17):13087–13097. [PubMed: 17331948]
14. Karacsonyi C, Miguel AS, Puertollano R. Mucolipin-2 Localizes to the Arf6-Associated Pathway and Regulates Recycling of GPI-APs. Traffic. 2007; 8(10):1404–1414. [PubMed: 17662026]
15. Lavezzari G, Roche KW. Constitutive endocytosis of the metabotropic glutamate receptor mGluR7 is clathrin-independent. Neuropharmacology. 2007; 52(1):100–107. [PubMed: 16890965]
16. Scarselli M, Donaldson JG. Constitutive internalization of G protein-coupled receptors and G proteins via clathrin-independent endocytosis. J Biol Chem. 2009 in press.

17. Walseng E, Bakke O, Roche PA. MHC class II-peptide complexes internalize using a clathrin -and dynamin-independent endocytosis pathway. J Biol Chem. 2008; 283:14717–14727. [PubMed: 18378669]

18. D'Souza-Schorey C, Chavrier P. ARF proteins: roles in membrane traffic and beyond. Nat Rev Mol Cell Biol. 2006; 7(5):347–358. [PubMed: 16633337]

19. Donaldson JG. Multiple roles for Arf6: Sorting, structuring, and signaling at the plasma membrane. Journal of Biological Chemistry. 2003; 278(43):41573–41576. [PubMed: 12912991]

20. Brown FD, Rozelle AL, Yin HL, Balla T, Donaldson JG. Phosphatidylinositol 4,5-bisphosphate and Arf6-regulated membrane traffic. J Cell Biol. 2001; 154(5):1007–1017. [PubMed: 11535619]

21. Weigert R, Yeung AC, Li J, Donaldson JG. Rab22a regulates the recycling of membrane proteins internalized independently of clathrin. Mol Biol Cell. 2004; 15(8):3758–3770. [PubMed: 15181155]

22. Caplan S, Naslavsky N, Hartnell LM, Lodge R, Polishchuk RS, Donaldson JG, Bonifacino JS. A tubular EHD1-containing compartment involved in the recycling of major histocompatibility complex class I molecules to the plasma membrane. Embo J. 2002; 21(11):2557–2567. [PubMed: 12032069]

23. Naslavsky N, Rahajeng J, Sharma M, Jovic M, Caplan S. Interactions between EHD proteins and Rab11-FIP2: a role for EHD3 in early endosomal transport. Mol Biol Cell. 2006; 17(1):163–177. [PubMed: 16251358]

24. Robertson SE, Setty SR, Sitaram A, Marks MS, Lewis RE, Chou MM. Extracellular signal-regulated kinase regulates clathrin-independent endosomal trafficking. Mol Biol Cell. 2006; 17(2): 645–647. [PubMed: 16314390]

25. Shi A, Pant S, Balklava Z, Chen CC, Figueroa V, Grant BD. A novel requirement for C. elegans Alix/ALX-1 in RME-1-mediated membrane transport. Curr Biol. 2007; 17(22):1913–1924. [PubMed: 17997305]

26. Balklava Z, Pant S, Fares H, Grant BD. Genome-wide analysis identifies a general requirement for polarity proteins in endocytic traffic. Nat Cell Biol. 2007; 9(9):1066–1073. [PubMed: 17704769]

27. Luo S, Wehr NB, Levine RL. Quantitation of protein on gels and blots by infrared fluorescence of Coomassie blue and Fast Green. Anal Biochem. 2006; 350(2):233–238. [PubMed: 16336940]

28. Porat-Shliom N, Kloog Y, Donaldson JG. A Unique Platform for H-Ras Signaling Involving Clathrin-independent Endocytosis. Mol Biol Cell. 2008; 19(3):765–775. [PubMed: 18094044]

29. Cichy J, Pure E. The liberation of CD44. J Cell Biol. 2003; 161(5):839–843. [PubMed: 12796473]

30. Gorter A, Meri S. Immune evasion of tumor cells using membrane-bound complement regulatory proteins. Immunol Today. 1999; 20(12):576–582. [PubMed: 10562709]

31. Deves R, Boyd CA. Surface antigen CD98(4F2): not a single membrane protein, but a family of proteins with multiple functions. J Membr Biol. 2000; 173(3):165–177. [PubMed: 10667913]

32. Iacono KT, Brown AL, Greene MI, Saouaf SJ. CD147 immunoglobulin superfamily receptor function and role in pathology. Exp Mol Pathol. 2007; 83(3):283–295. [PubMed: 17945211]

33. Holman GD, Kozka IJ, Clark AE, Flower CJ, Saltis J, Habberfield AD, Simpson IA, Cushman SW. Cell surface labeling of glucose transporter isoform GLUT4 by bis-mannose photolabel. Correlation with stimulation of glucose transport in rat adipose cells by insulin and phorbol ester. J Biol Chem. 1990; 265(30):18172–18179. [PubMed: 2211693]

34. Wu WW, Wang G, Yu MJ, Knepper MA, Shen RF. Identification and quantification of basic and acidic proteins using solution-based two-dimensional protein fractionation and label-free or 18O-labeling mass spectrometry. J Proteome Res. 2007; 6(7):2447–2459. [PubMed: 17506541]

35. Wang G, Wu WW, Zeng W, Chou CL, Shen RF. Label-free protein quantification using LC-coupled ion trap or FT mass spectrometry: Reproducibility, linearity, and application with complex proteomes. J Proteome Res. 2006; 5(5):1214–1223. [PubMed: 16674111]

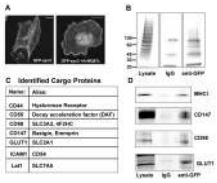

Figure 1.

Immunoisolation of Arf6Q67L-induced vacuoles and cargo protein identification. A. Localization of GFP-syntaxin 3 (GFP-syn3) in Hela cells alone (left) and in cells co-expressing Arf6Q67L (right). Bar, 10 μm. B. Coomassie blue staining of cell lysate, material bound to IgG beads and material bound to anti-GFP beads. C. List of cargo proteins identified by LC/MS/MS. D. Immunoblot of lysate and material bound to beads using antibodies to MHCI, CD147, CD98 and Glut1. For the lysate 25-50 mg of cellular lysate was loaded and for the bound approximately 5-10% of the bound material was loaded onto the gels.

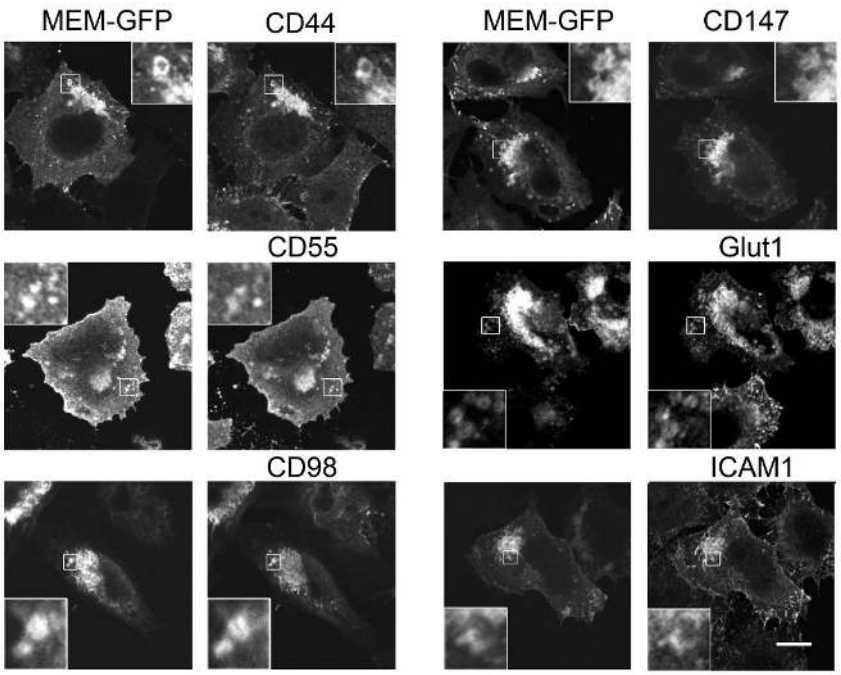

Figure 2.

New cargo proteins localize to Arf6Q67L vacuoles. HeLa cells co-expressing Arf6Q67L and Mem-GFP were fixed and then distribution of the cargo proteins was revealed with antibodies directed against CD44, CD55, CD98, CD147, Glut1, and ICAM1, followed by 594-conjugated goat-anti-mouse and goat-anti-rabbit (for Glut1). Bar, 10 μm.

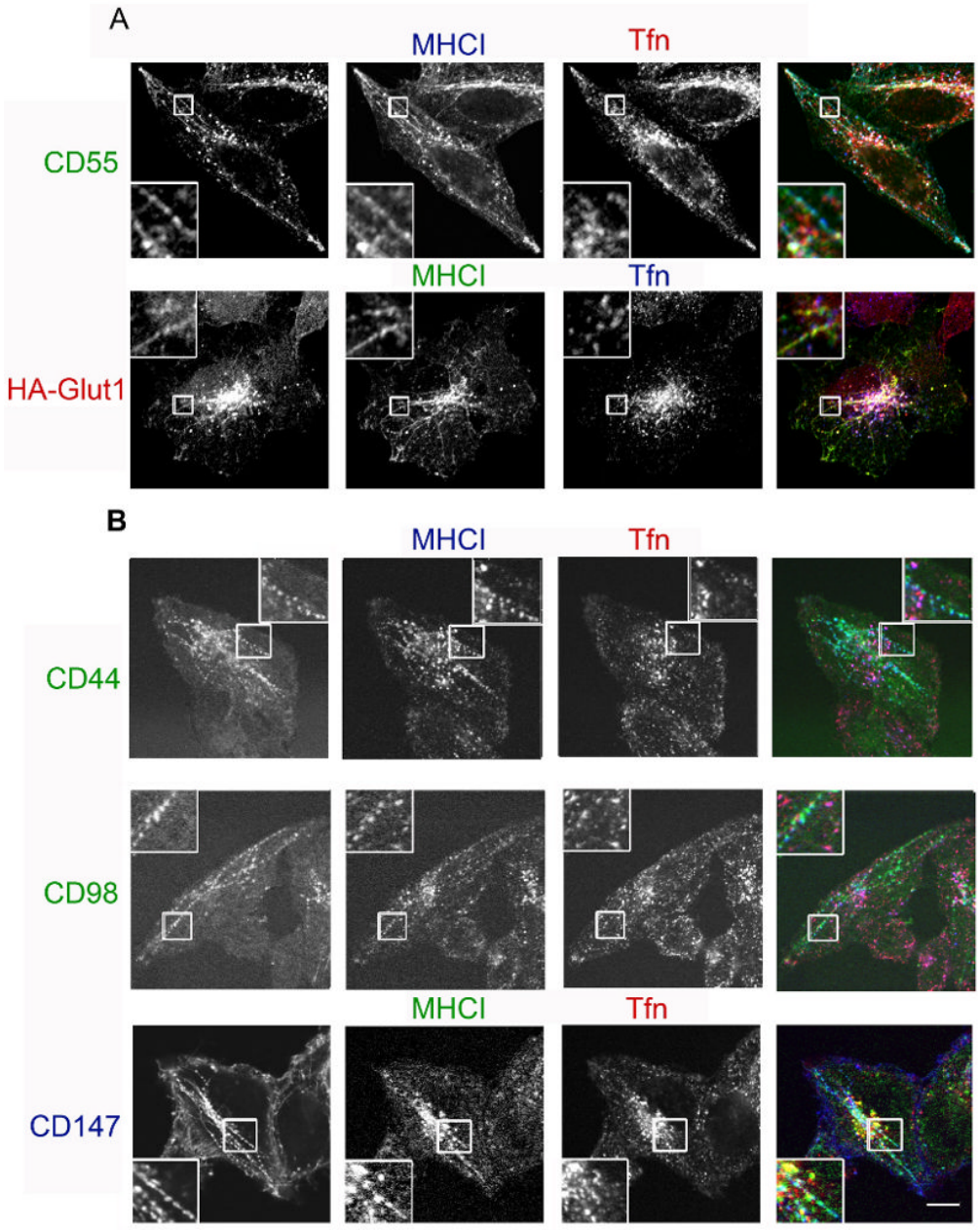

Figure 3.

New cargo proteins differ in their intracellular trafficking. Cells were incubated with monoclonal antibodies directed towards CD55, HA-Glut1, CD44, CD98 and CD147 in the presence of antibodies to MHCI and labeled transferrin for 60 min. For A, unlabelled antibodies were used for internalization and, after fixation, surface antibody was blocked with unlabeled goat-anti-mouse IgG, followed by fluorescently conjugated isotype-specific secondary antibodies in the presence of saponin. In B, directly conjugated antibodies were used and after incubation, surface-bound antibody was removed by acid wash prior to fixation. Bar, 10μm.

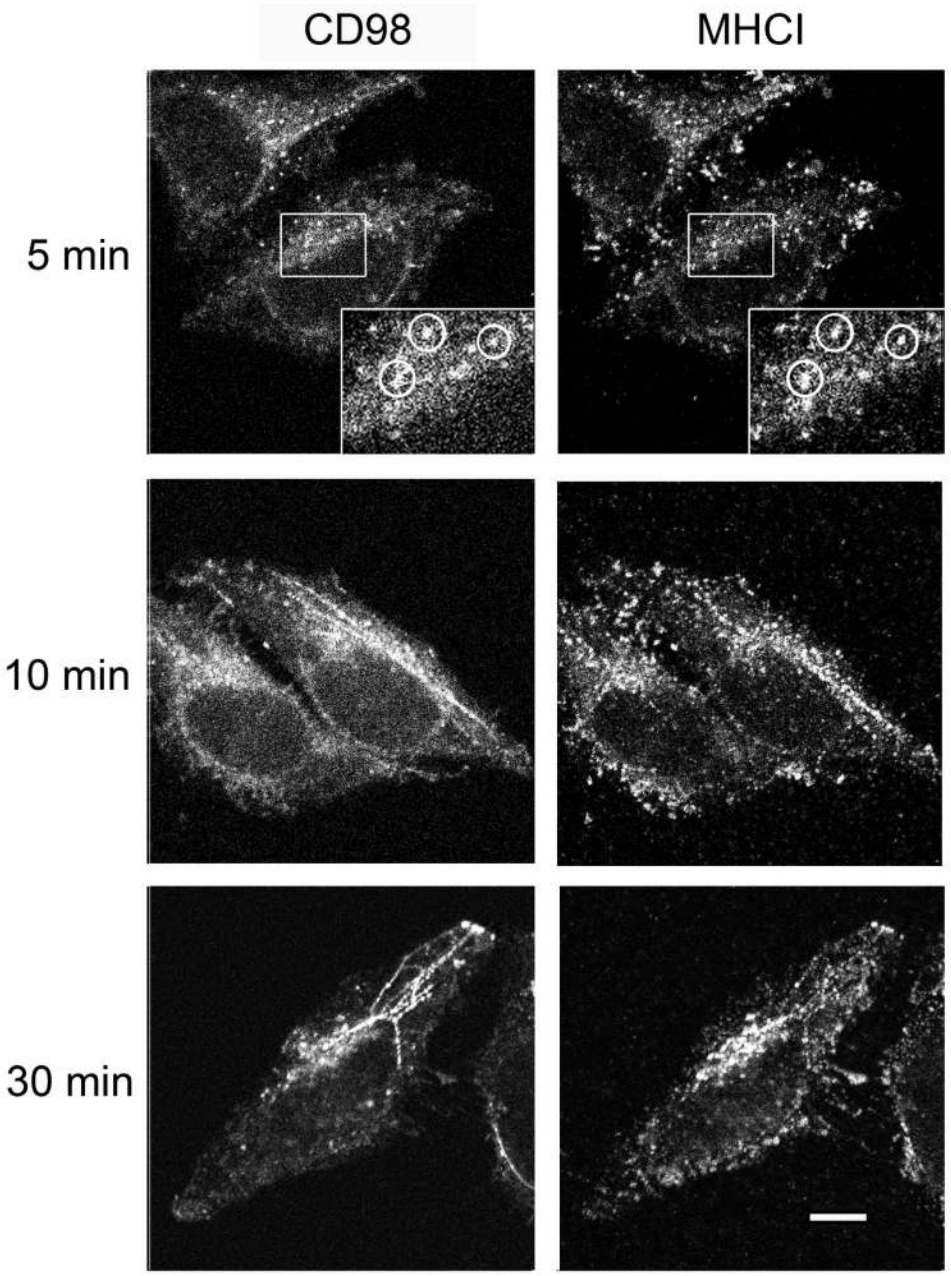

Figure 4.
CD98 and MHCI colocalize at short times of internalization. HeLa cells were incubated with directly conjugated monoclonal antibodies to CD98 and MHCI for 5, 10 and 30 min and then surface antibody was removed by acid wash prior to fixation. Bar, 10μm.

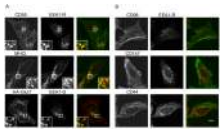

Figure 5.
CD55, Glut1 and MHCI reach, whereas CD98, CD147 and CD44 do not reach, EEA1-positive compartments. Unlabeled antibodies to CD55, HA, MHCI, CD98, and CD147 were incubated with cells for 30 min to allow internalization. After removal of free antibody, cells were fixed and surface-bound antibody was blocked with unlabeled goat-anti-mouse IgG. Cells were then incubated in the presence of saponin with rabbit-anti-EEA1 antibody, followed by secondary antibodies to detect EEA1 and the internalized cargo proteins. For CD44 internalization, 488-CD44 antibody was used for internalization and prior to fixation the cells were treated with low pH wash to remove surface antibody. Bar, 10 μm.

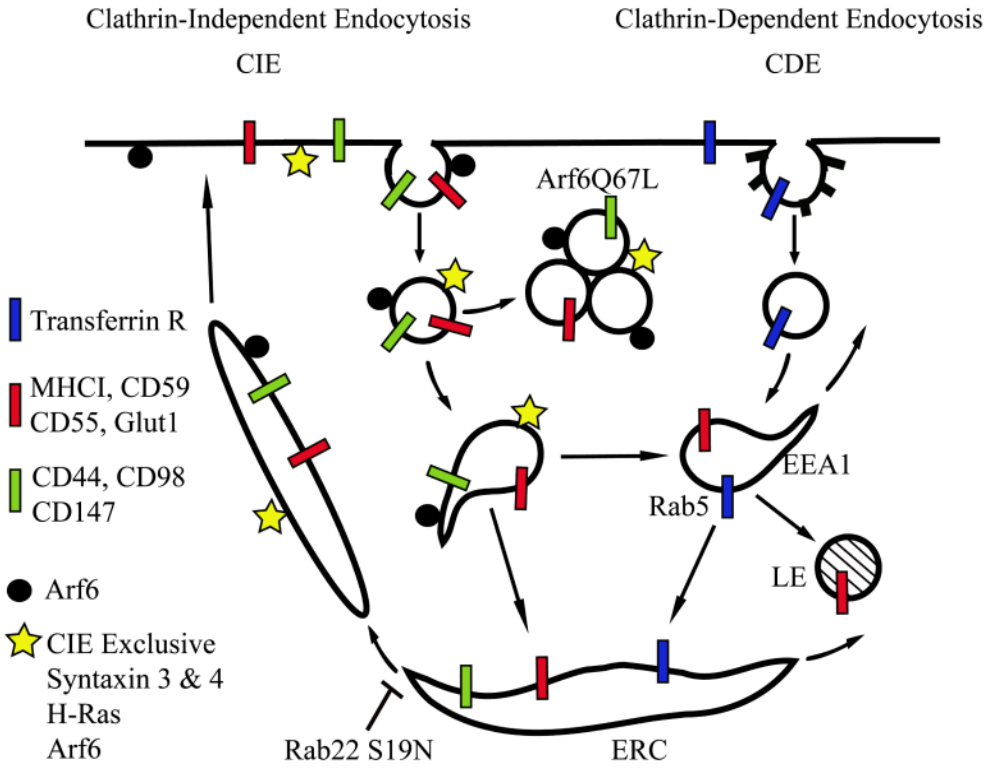

Figure 6.

Model showing possible sorting within the CIE pathway in HeLa cells. Trafficking of CIE (red and green bars) and CDE (blue bars) cargo proteins. Some CIE cargo (red bars) traffics along with MHCI to EEA1 early endosomes en route to late endosomes (LE) or to recycling via the endosomal recycling compartment (ERC). Other CIE cargo (green bars) take a more direct route via the ERC to the tubular recycling compartment and are largely absent from the EEA1-positive early endosome.